DS-CDMA Downlink Site Diversity with Frequency-Domain Equalization and Antenna Diversity Reception

Hirotaka SATO[†], Hiromichi TOMEBA[†a)], Kazuaki TAKEDA[†], *Student Members*, *and* Fumiyuki ADACHI[†], *Fellow*

SUMMARY   The use of frequency-domain equalization based on minimum mean square error criterion (called MMSE-FDE) can significantly improve the bit error rate (BER) performance of DS-CDMA signal transmission compared to the well-known coherent rake combining. However, in a DS-CDMA cellular system, as a mobile user moves away from a base station and approaches the cell edge, the received signal power gets weaker and the interference from other cells becomes stronger, thereby degrading the transmission performance. To improve the transmission performance of a user close to the cell edge, the well-known site diversity can be used in conjunction with FDE. In this paper, we consider DS-CDMA downlink site diversity with FDE. The MMSE site diversity combining weight is theoretically derived for joint FDE and antenna diversity reception and the downlink capacity is evaluated by computer simulation. It is shown that the larger downlink capacity can be achieved with FDE than with coherent rake combining. It is also shown that the DS-CDMA downlink capacity is almost the same as MC-CDMA downlink capacity.
key words: *DS-CDMA, frequency-domain equalization, site diversity, link capacity*

1. Introduction

Direct sequence code division multiple access (DS-CDMA) with coherent rake combining is used in third generation (3G) mobile communication systems that provide data services of up to a few Mbps [1]. In coherent rake receivers, the copies of the transmitted signal propagated through different paths are coherently combined to obtain the path diversity gain and improve the bit error rate (BER) performance. Lately, there have been strong demands for extremely higher speed data transmissions than 3G systems [2]. The forth generation (4G) mobile communication systems are expected to emerge around 2010 or later. In 4G systems, 100 Mbps–1 Gbps class data transmission is said to be necessary. However, since the channel becomes severely frequency-selective [3], the BER performance of DS-CDMA with coherent rake combining significantly degrades due to strong inter-path interference (IPI). Recently, it was shown [4] that the use of frequency-domain equalization based on minimum mean square error criterion (called MMSE-FDE) can significantly improve the BER performance compared to coherent rake combining and achieve a BER performance similar to multicarrier CDMA (MC-

CDMA). Moreover, antenna diversity reception is effective to improve the transmission performance.

However, in a cellular mobile communication system, as a mobile user moves, the local average received signal power slowly varies in time due to distance-dependent path loss and shadowing loss [3]. The performance degradation owing to this slow variation gets severer as a mobile station (MS) approaches the cell edge where the received signal power is weak and the interference from other cells is strong. Since the same carrier frequency is used in a DS-CDMA cellular system, sufficient signal power can be obtained by transmitting the same signal simultaneously from different base stations (BS's) surrounding the MS [5]. This technique is called site diversity.

So far, MC-CDMA downlink site diversity was studied in [6]. However, to the best of author's knowledge, no literature is found for DS-CDMA downlink site diversity with FDE. In this paper, we theoretically derive the MMSE site diversity combining weight for DS-CDMA downlink with joint FDE and antenna diversity reception. We evaluate the downlink capacity by computer simulation and show that DS-CDMA can achieve almost the same downlink capacity as MC-CDMA. The remainder of this paper is organized as follows. Section 2 presents the DS-CDMA downlink site diversity with joint FDE and antenna diversity reception. In Sect. 3, the MMSE site diversity combining weight is theoretically derived. The simulation results are presented and discussed in Sect. 4. Section 5 gives some conclusion of this paper and future work.

2. DS-CDMA Downlink Site Diversity with FDE and Antenna Diversity Reception

2.1 Site Diversity Model

Figure 1 shows the downlink site diversity model. In the downlink site diversity, as the number of base stations (active BS's) participating in site diversity increases, a larger interference is produced and degrades the downlink capacity. Therefore, the selection method of active BS's is important.

Assuming that all BS's are transmitting their pilot signals with equal power, each MS measures the local average received signal powers from its surrounding BS's and sorts out them in descending order for the selection of active BS's. A BS giving a local average received signal power within the

Fig. 1 Downlink site diversity model.

(a) Transmitter (BS i).

(b) Receiver (MS u).
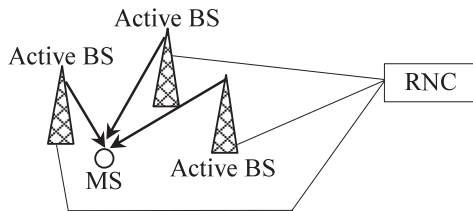
Fig. 2 Transmitter/receiver structure.

Fig. 3 Block structure.

inserted into the guard interval (GI) placed at the beginning of the block as a cyclic prefix. Figure 3 illustrates the block structure.

In this paper, we consider the transmission of one block without loss of generality and the chip-spaced time representation of the signals is used. The equivalent lowpass representation $\tilde{s}_i(t)$ of the downlink signal of BS i can be expressed as

$$\tilde{s}_i(t) = \sqrt{\frac{2E_c}{T_c}} s_i(t), \tag{1}$$

where E_c is the chip energy per user, T_c is the chip duration and

$$s_i(t) = \left[\sum_{u=0}^{U_i-1} d_u \left(\lfloor t/SF \rfloor \right) c_u \left(t \bmod SF \right) \right] c_{scr(i)}(t), \tag{2}$$

where $\lfloor x \rfloor$ represents the largest integer smaller than or equal to x.

(2) Received signal representation

The transmitted signal is received by M antennas at MS u via a frequency-selective fading channel. We assume an L-path fading channel, between BS i and receive antenna m ($m = 0 \sim M - 1$) at MS u, with impulse response $h_{i\_u}^{(m)}(t)$ given as [8]

$$h_{i\_u}^{(m)}(t) = \sum_{l=0}^{L-1} h_{i\_u,l}^{(m)} \delta(t - \tau_l), \tag{3}$$

where $\{h_{i\_u,l}^{(m)}; \; l = 0 \sim L - 1\}$ is the lth path gain with $\sum_{l=0}^{L-1} E[|h_{i\_u,l}^{(m)}|^2] = 1$ ($E[.]$ denotes the ensemble average) and τ_l is the T_c-spaced time delay of lth path.

The received signal $r_u^{(m)}(t)$ on the antenna m at MS u can be expressed as

$$r_u^{(m)}(t) = \sum_{i=0}^{\infty} \sqrt{\frac{2E_{c,i\_u}}{T_c}} \left[\sum_{l=0}^{L-1} h_{i\_u,l}^{(m)} s_i(t - \tau_l) \right] + \eta^{(m)}(t), \tag{4}$$

where E_{c,i_u} is the local average received chip energy when the signal transmitted from BS i is received at MS u. E_{c,i_u} is expressed as

$$E_{c,i\_u} = E_c \cdot R_{i\_u}^{-\alpha} \cdot 10^{-\delta_{i\_u}/10}, \tag{5}$$

where R_{i_u} is the distance between BS i and MS u, α is the path loss exponent, δ_{i_u} is the log-normally distributed shadowing loss and $\eta^{(m)}(t)$ is the zero mean additive white Gauss noise (AWGN) process with variance $2N_0/T_c$ (N_0 is the single-sided power spectrum density).
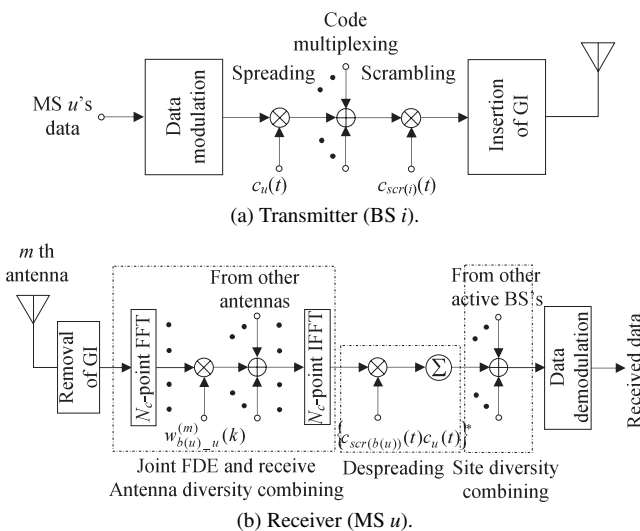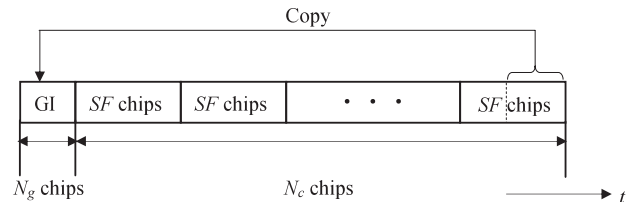
threshold P_{th} dB from the maximum power will be selected as an active BS. All active BS's transmit the same signal simultaneously to the MS. If $P_{th} = 0$ dB, the MS communicates with only one BS giving the maximum local average received signal power (i.e., without site diversity). The radio network controller (RNC) monitors the whole site diversity operation [7].

2.2 Downlink Transmission Model

Figure 2 shows the BS transmitter/MS receiver structure. An active BS transmitting to the MS u is denoted by BS $b(u)$. The maximum number of active BS's is limited to D_{max}.

(1) Transmit signal representation

Assume that BS i is communicating with U_i users. A binary data sequence to be transmitted to MS u is transformed into a data symbol sequence $\{d_u(n); \; n = \ldots, -1, 0, 1, \ldots\}$. After U_i data symbol sequences $\{d_u(n); \; n = 0 \sim N_c/SF - 1\}$, $u = 0 \sim U_i - 1$, are spread by orthogonal spreading codes $\{c_u(t); \; t = 0 \sim SF - 1\}$, $u = 0 \sim U_i - 1$, having a spreading factor SF, they are code multiplexed and then multiplied by a BS-specific scrambling code $\{c_{scr(i)}(t); \; t = 0 \sim N_c - 1\}$.

The resulting chip sequence is divided into a sequence of chip blocks of N_c chips each, where N_c is the block size (in chips) for fast Fourier transform (FFT) at a mobile receiver. N_c is chosen so that the value of N_c/SF becomes an integer. The last N_g chips of the N_c-chip block is copied and

(3) Site diversity combining with FDE and antenna diversity reception

At MS u, after the removal of the GI, the received signal is decomposed into N_c subcarrier components by N_c-point FFT. The kth subcarrier component $R_u^{(m)}(k)$ is given by

$$
\begin{aligned}
R_u^{(m)}(k) &= \sum_{t=0}^{N_c-1} r_u^{(m)}(t) \exp\left(-j2\pi k \frac{t}{N_c}\right) \\
&= \sum_{i=0}^{\infty} \left[\sqrt{\frac{2E_{c,i\_u}}{T_c}} H_{i\_u}^{(m)}(k) S_i(k) \right] + \Pi^{(m)}(k), \quad (6)
\end{aligned}
$$

where $S_i(k)$ is the kth subcarrier component of $s_i(t)$, $H_{i\_u}^{(m)}(k)$ is the kth subcarrier channel gain of the multipath channel between BS i and MS u and $\Pi^{(m)}(k)$ is the kth subcarrier component of $\eta^{(m)}(t)$. They are written as

$$
\left\{
\begin{aligned}
S_i(k) &= \sum_{t=0}^{N_c-1} s_i(t) \exp\left(-j2\pi k \frac{t}{N_c}\right) \\
H_{i\_u}^{(m)}(k) &= \sum_{l=0}^{L-1} h_{i\_u,l}^{(m)} \exp\left(-j2\pi k \frac{\tau_l}{N_c}\right) \\
\Pi^{(m)}(k) &= \sum_{t=0}^{N_c-1} \eta^{(m)}(t) \exp\left(-j2\pi k \frac{t}{N_c}\right)
\end{aligned}
\right. \quad (7)
$$

Joint FDE and receive antenna diversity combining is performed on $\{R_u^{(m)}(k); k = 0 \sim N_c - 1\}$ as

$$
\hat{R}_{b(u)\_u}(k) = \sum_{m=0}^{M-1} w_{b(u)\_u}^{(m)}(k) R_u^{(m)}(k), \quad (8)
$$

where $w_{b(u)\_u}^{(m)}(k)$ is the MMSE weight associated with the active BS $b(u)$ (which will be derived in Sect. 3). By applying N_c-point inverse FFT (IFFT), the time-domain chip sequence $\hat{r}_{b(u)\_u}(t)$ after joint FDE and receive antenna diversity combining is obtained as

$$
\hat{r}_{b(u)\_u}(t) = \frac{1}{N_c} \sum_{k=0}^{N_c-1} \hat{R}_{b(u)\_u}(k) \exp\left(j2\pi k \frac{t}{N_c}\right). \quad (9)
$$

Then, despreading is carried out on $\hat{r}_{b(u)\_u}(t)$ to get the decision variable $\hat{d}_{b(u)\_u}(n)$ associated with the active BS $b(u)$ for the transmitted symbol $d_u(n)$ as

$$
\begin{aligned}
\hat{d}_{b(u)\_u}(n) &= \frac{1}{SF} \sum_{t=nSF}^{(n+1)SF-1} \hat{r}_{b(u)\_u}(t) \\
&\times \{c_{scr(b(u))}(t) c_u(t \bmod SF)\}^*. \quad (10)
\end{aligned}
$$

Finally, the decision variables associated with all active BS's are combined to obtain the site diversity-combined decision variable as

$$
\tilde{d}_u(n) = \sum_{b(u)=0}^{D-1} \hat{d}_{b(u)\_u}(n), \quad (11)
$$

where D $(1 \leq D \leq D_{\max})$ is the number of active BS's. Data demodulation is done on $\{\tilde{d}_u(n); n = 0 \sim N_c/SF - 1\}$ to recover the transmitted binary data sequence of N_c/SF symbols.

3. MMSE Weight Derivation

In order to derive the MMSE site diversity combining weight for DS-CDMA downlink with joint FDE and antenna diversity reception, we assume $P_{th} \to \infty$ and that all BS's are participating in site diversity $(D_{\max} \to \infty)$ [6]. Substituting Eq. (10) into Eq. (11) gives

$$
\begin{aligned}
\tilde{d}_u(n) &= \frac{1}{SF} \sum_{t=nSF}^{(n+1)SF-1} \left[\sum_{b(u)=0}^{\infty} \hat{r}_{b(u)\_u}(t) \right] \\
&\times \{c_{scr(b(u))}(t) c_u(t \bmod SF)\}^*. \quad (12)
\end{aligned}
$$

The kth subcarrier component $\tilde{R}_u(k)$ of $\sum_{b(u)=0}^{\infty} \hat{r}_{b(u)\_u}(t)$ is given, from Eqs. (8) and (9), as

$$
\begin{aligned}
\tilde{R}_u(k) &= \sum_{b(u)=0}^{\infty} \sum_{m=0}^{M-1} w_{b(u)\_u}^{(m)}(k) \\
&\times \left[\sum_{i=0}^{\infty} \left(\sqrt{\frac{2E_{c,i\_u}}{T_c}} H_{i\_u}^{(m)}(k) S_i(k) \right) + \Pi^{(m)}(k) \right]. \quad (13)
\end{aligned}
$$

Let's define the equalization error at the kth subcarrier as

$$
e_u(k) = \tilde{R}_u(k) - \tilde{S}_u(k), \quad (14)
$$

where $\tilde{S}_u(k)$ is the kth subcarrier component in the sum of transmitted signals from all active BS's and it is written as

$$
\tilde{S}_u(k) = \sum_{b(u)=0}^{\infty} \left[\sqrt{\frac{2E_{c,b(u)\_u}}{T_c}} S_{b(u)\_u}(k) \right] \quad (15)
$$

with

$$
\begin{aligned}
S_{b(u)\_u}(k) &= \sum_{t=0}^{N_c-1} [d_u(\lfloor t/SF \rfloor) c_u(t \bmod SF) c_{scr(b(u))}(t)] \\
&\times \exp\left(-j2\pi k \frac{t}{N_c}\right). \quad (16)
\end{aligned}
$$

Using Eqs. (13) and (15), the mean square error $E[|e_u(k)|^2]$ is given as

$$
\begin{aligned}
E\left[|e_u(k)|^2\right] &= E\left[\left|\tilde{R}_u(k) - \tilde{S}_u(k)\right|^2\right] \\
&= \sum_{b(u)=0}^{\infty} E\left[\left|e_{b(u)}(k)\right|^2\right], \quad (17)
\end{aligned}
$$

where

$$
\begin{aligned}
e_{b(u)}(k) &= \sum_{m=0}^{M-1} w_{b(u)\_u}^{(m)}(k) \left[\sum_{i=0}^{\infty} \left(\sqrt{\frac{2E_{c,i\_u}}{T_c}} H_{i\_u}^{(m)}(k) S_i(k) \right) + \Pi^{(m)}(k) \right] \\
&\quad - \sqrt{\frac{2E_{c,b(u)\_u}}{T_c}} S_{b(u)\_u}(k). \quad (18)
\end{aligned}
$$

The MMSE weight can be found from

$$\frac{\partial}{\partial w_{b(u)\_u}^{(m)}(k)} E\left[\left| e_{b(u)}(k) \right|^2 \right] = 0. \tag{19}$$

Substituting Eq. (18) into Eq. (19) gives

$$\sum_{i=0}^{\infty} U_i \Gamma_{i\_u} \left\{ H_{i\_u}^{(m)}(k) \right\}^* \left[\sum_{m'=0}^{M-1} w_{b(u)\_u}^{(m')}(k) H_{i\_u}^{(m')}(k) \right]$$
$$+ SF \cdot w_{b(u)\_u}^{(m)}(k) - \Gamma_{b(u)\_u} \left\{ H_{b(u)\_u}^{(m)}(k) \right\}^* = 0, \tag{20}$$

where $\Gamma_{b(u)\_u}$ is the local average received signal energy per symbol-to-the AWGN power spectrum density ratio for the signal transmitted from BS $b(u)$ and is given by

$$\Gamma_{b(u)\_u} = \frac{SF \cdot E_c (1 + N_g/N_c)^{-1}}{N_0} R_{b(u)\_u}^{-\alpha} 10^{-\delta_{b(u)\_u}/10}. \tag{21}$$

We have assumed that the data symbol sequences $\{d_u(n)\}$, $u = 0 \sim U_i - 1$, are independent and random. From Eq. (20) and after some manipulations similar to [6], we can show that the MMSE weight is given as

$$w_{b(u)\_u}^{(m)}(k) = \frac{\Gamma_{b(u)\_u} \left\{ H_{b(u)\_u}^{(m)}(k) \right\}^*}{\sum_{i=0}^{\infty} U_i \Gamma_{i\_u} \left[\sum_{m'=0}^{M-1} \left| H_{i\_u}^{(m')}(k) \right|^2 \right] + SF}. \tag{22}$$

4. Computer Simulation

4.1 Simulation Conditions and Procedure

Figure 4 shows a cellular structure considered in the computer simulation. Each cell is illuminated by a BS with omnidirectional antenna. An MS of interest is located in the center cell (i = 0th cell). Each MS is assumed to receive the signals transmitted from only 7 surrounding BS's and interference-limited environment is assumed. Table 1 shows the simulation condition. We assume QPSK data modulation, an FFT window size of N_c = 256 chips and a GI length of N_g = 32 chips. Both channel estimation and local average received signal power estimation are ideally performed. The path loss exponent α is set to α = 3–4 and the standard deviation of shadowing loss σ is set to σ = 6 dB. Fading is assumed to be a block Rayleigh fading having an L = 16-path uniform power delay profile with $\tau_l = l$ chips (l= $0 \sim L - 1$) so that the path gains remain constant over one block interval of N_c chips. The threshold P_{th} is set to P_{th} = 0–10 dB, the required BER is set to 10^{-2} and the allowable outage probability P_o is set to P_o = 10%. We use D_{max} = 7.

Computer simulation is performed by the following procedure. Starting from $U = 1$, U MS's locations in each cell are randomly generated, followed by the generation of shadowing loss δ_{i_u} and path gains $\{h_{i\_u,l}^{(m)}; l = 0 \sim L - 1, m = 0 \sim M - 1\}$. Each MS measures the local average received signal power from each BS to select active BS's, each giving
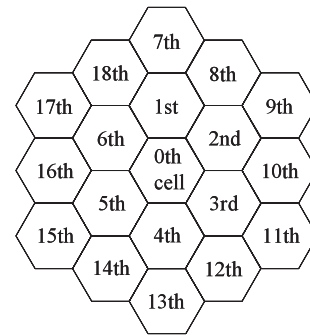

Fig. 4　Cellular structure.

Table 1　Simulation conditions.

DS-CDMA transmitter/ receiver	Data modulation	QPSK
	No. of FFT points	N_c=256
	GI lengths	N_g=32
	Spreading code	Walsh-Hadamard code
	Scrambling code	Long PN code
	Spreading factor	SF=256
	Frequency-domain equalization	MMSE
	Channel estimation	Ideal
	No. of receive antennas	M=1~4
Channel model	Path loss exponent	α=3~4
	Standard deviation of shadowing loss	σ=6dB
	Fading	Block Rayleigh fading
	No. of paths	L=1~32
	Power delay profile	Uniform
Site diversity	User distribution	Uniform
	Threshold	P_{th}=0~10dB
	Maximum no. of active BS's	D_{max}=7
Link quality requirement	Required BER	10^{-2}
	Allowable outage probability	P_o=10%

the local average received signal power within the threshold P_{th} dB from the maximum. After selecting the active BS's, the number U_i of data channels of BS i is determined. Performing the signal transmission described in Sect. 2, the BER measurement of the MS is carried out. After having measured the local average BER, locations of all MS's are changed to measure the local average BER again. This measurement process is repeated a sufficient number of times to find the distribution of the local average BER. If the probability (outage probability) of the local average BER being larger than the required BER is smaller than P_o, the number U of MS is incremented by one (i.e. $U + 1 \to U$). The downlink capacity U_{max} is defined as the maximum number of MS that keeps the outage probability smaller than P_o.

In this paper, we compare the DS-CDMA downlink capacity with the MC-CDMA downlink capacity. For a fair comparison, the same simulation conditions as in DS-CDMA are assumed, i.e., QPSK data modulation, MC-
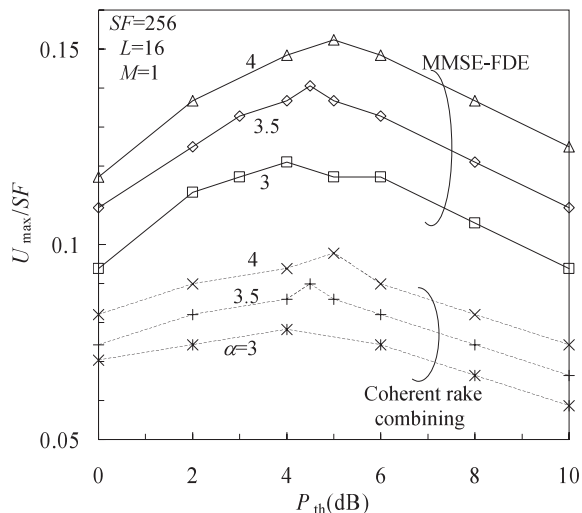
Fig. 5   Effect of site diversity threshold P_{th}.

Fig. 6   Probability of the number D of active BS's.

Fig. 7   Effect of the number M of receive antennas.

CDMA with $N_c = 256$ subcarriers, a GI length of $N_g = 32$ samples, and a spreading factor $SF = 256$. The difference between MC-CDMA and DS-CDMA is the placement of an N_c-point IFFT operation; it is used at the receiver in DS-CDMA as in Fig. 2, but it is used before the GI insertion at the transmitter in MC-CDMA [4]. The selection method of active BS's is the same as in DS-CDMA.

4.2   Results and Discussion

The normalized downlink capacity U_{max}/SF is plotted in Fig. 5 as a function of the threshold P_{th}. As P_{th} increases, the normalized downlink capacity increases since the number of active BS's increases and larger site diversity gain is obtained. However, when P_{th} exceeds a certain value, the normalized downlink capacity decreases due to the excessive interference because too many active BS's are involved. It is seen from Fig. 5 that the maximum downlink capacity is about 1.3 times larger than without site diversity ($P_{th} = 0$ dB). As the path loss exponent α increases, the optimum P_{th} that maximizes the downlink capacity increases. This is because P_{th} needs to be increased to get more active BS's for site diversity operation. The optimum P_{th} is found to be around 4–5 dB when $\alpha = 3$–4. The downlink capacity increases as α gets larger, since, as α gets larger, the interference signals are attenuated more and the signal-to-interference power ratio (SIR) gets larger. It is also seen from Fig. 5 that the downlink capacity with MMSE-FDE is larger than that with coherent rake combining since MMSE-FDE can significantly reduce the IPI; the maximum downlink capacity with MMSE-FDE is about 1.6 times larger than with coherent rake combining.

The probability of the number D of active BS's is plotted in Fig. 6 when $\alpha = 3.5$. As P_{th} increases, the probability of $D = 4$–6 becomes larger. This suggests that the inter-code interference gets severer if too large P_{th} is used. When the optimum P_{th} (≈ 4.5 dB) is used, a sufficient signal power can be collected by site diversity and excessive interference
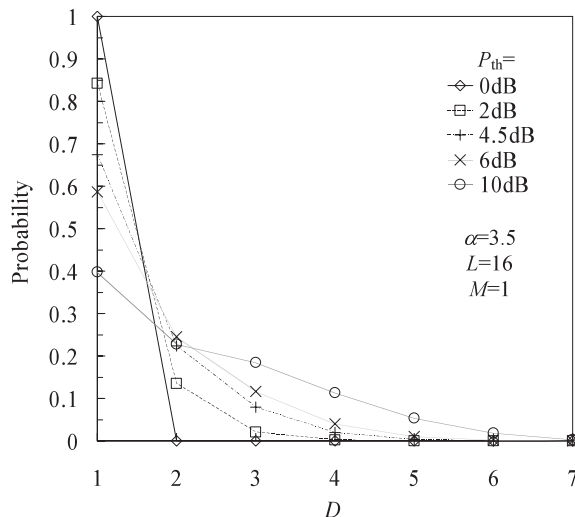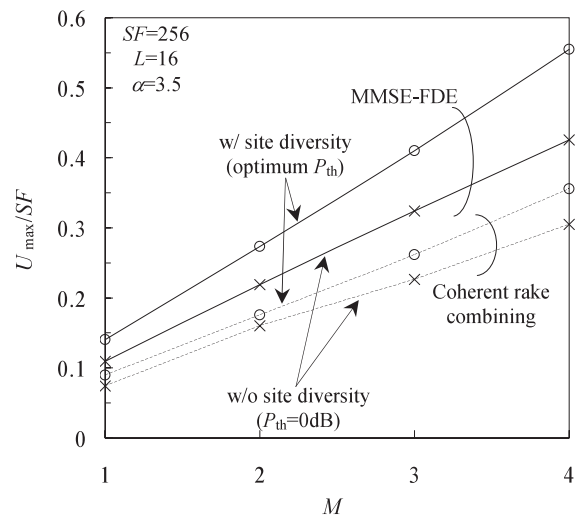
is avoided due to the small probability of $D = 4$–7.

Figure 7 shows the effect of the number M of receive antennas on the downlink capacity, where the optimum P_{th} (the optimum P_{th} was found to be almost the same with and without antenna diversity reception) and $P_{th} = 0$ dB (without site diversity) are used. The joint use of MMSE-FDE and antenna diversity reception is very effective to improve the downlink capacity. The downlink capacity linearly increases with M.

Figure 8 plots the normalized downlink capacity with site diversity using the optimum P_{th} and that without site diversity ($P_{th} = 0$ dB) as a function of the number L of paths. MMSE-FDE always provides better downlink capacity than coherent rake combining. As L increases, the downlink capacity of MMSE-FDE improves since larger frequency diversity gain can be obtained. However, the downlink capacity approaches the upper limit for $L > 16$. In the case of coherent rake combining, as L increases from $L = 1$ to L
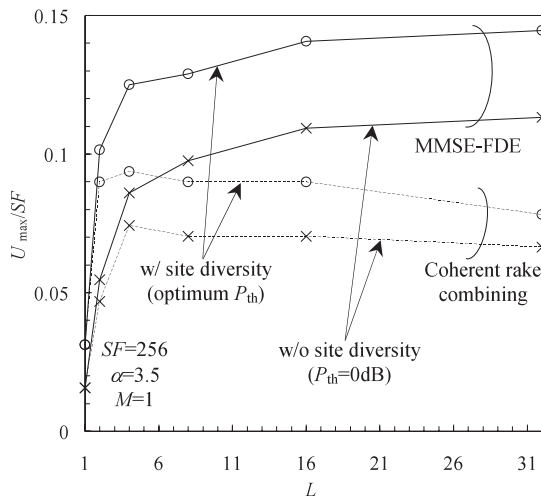
Fig. 8 Effect of the number L of paths.

Fig. 9 Downlink capacity comparison between DS-CDMA and MC-CDMA.

= 4, the normalized downlink capacity with coherent rake combining also increases due to increasing path diversity gain. However, as L increases beyond $L = 4$, large IPI is produced and it reduces the downlink capacity. When $L = 4$ (16), MMSE-FDE gives about 1.3 (1.6) times larger downlink capacity than coherent rake combining.

The downlink capacities of both DS-CDMA and MC-CDMA, with site diversity using MMSE-FDE, are compared in Fig. 9. It is seen that the optimum P_{th} is the same for both CDMA schemes. With the optimum P_{th}, the DS-CDMA downlink capacity is almost the same as MC-CDMA. The reason for this is given below. When $N_c = SF = 256$, since the data symbol to be transmitted is spread over all N_c subcarriers in both MC- and DS-CDMA, the same frequency diversity gain can be obtained in them, leading to the same downlink capacity for them.

When site diversity is used, the receiver complexity increases. Below, we present the complexity comparison in terms of the number of complex multiplications per block of N_c chips. In the receiver, N_c-point FFT (the number of complex multiplications is $N_c \log_2 N_c$) and FDE (the number of complex weight multiplications is N_c) are performed on each antenna. At the receiver, after M-antenna diversity combining, N_c-point IFFT (the number of complex multiplications is $N_c \log_2 N_c$) and despreading (the number of complex multiplications is N_c) are performed for each of D ($1 \le D \le D_{max}$) base stations participating in site diversity. As a result, the total number N of complex multiplications is

$$N = \{(N_c \log_2 N_c + N_c)M + N_c \log_2 N_c + N_c\} D$$
$$= (M + 1)(N_c \log_2 N_c + N_c)D. \qquad (23)$$

Obviously, the number of complex multiplications is proportional to D. Therefore, the downlink capacity improvement by using site diversity can be achieved at the cost of complexity increase. However, it can be seen from Fig. 6 that when the optimum P_{th} (≈ 4.5 dB) is used, the probability of the number D of active BS's is about 67.4% for $D =$
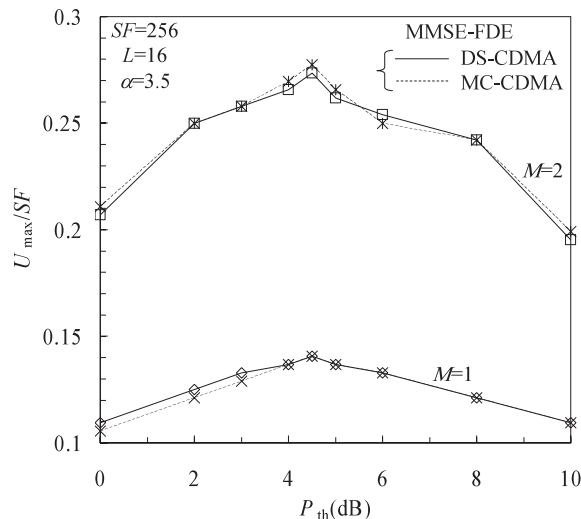
1, 22.3% for $D = 2$, 7.9% for $D = 3$ and 2.3% for $D = 4$–7. Hence, D_{max} can be set to 2–3 to get a sufficient capacity increase (D_{max} was set to 7 in the computer simulation).

5. Conclusion

In this paper, we theoretically derived the MMSE site diversity combining weight for DS-CDMA downlink with joint FDE and antenna diversity reception. It was shown by computer simulation that site diversity with MMSE-FDE provides a downlink capacity about 1.6 times larger than with coherent rake combining. It was also shown that the joint use of MMSE-FDE and antenna diversity reception increases the capacity and that DS-CDMA can achieve almost the same downlink capacity as MC-CDMA.

In this paper, we have considered downlink site diversity for uncoded DS- and MC-CDMA cellular systems. The discussion about the link capacity of coded DS-CDMA site diversity with FDE is left as a future study. Site diversity can also be applied to orthogonal frequency division multiplexing (OFDM) cellular system. However, it is necessary to consider some subcarrier allocation method or scheduling method. The implementation of site diversity for OFDM cellular system is not easy. Therefore, in this paper, we did not consider OFDM site diversity. OFDM site diversity is also left as an interesting future study.

References

[1] F. Adachi, M. Sawahashi, and H. Suda, "Wideband DS-CDMA for next generation mobile communications systems," IEEE Commun. Mag., vol.36, no.9, pp.56–69, Sept. 1998.

[2] Y. Kim, B.J. Jeong, J. Chung, C. Hwang, J.S. Ryu, K. Kim, and Y. Kim, "Beyond 3G: Vision, requirements, and enabling technologies," IEEE Commun. Mag., vol.41, no.3, pp.120–124, March 2003.

[3] W.C. Jakes, Jr., ed., Microwave Mobile Communications, Wiley, New York, 1974.

[4] F. Adachi, D. Garg, S. Takaoka, and K. Takeda, "Broadband CDMA

techniques," IEEE Wireless Commun. Mag., vol.12, no.2, pp.8–18, April 2005.

[5] A.J. Viterbi, CDMA: Principles of spread spectrum communications, Addison-Wesley, 1995.

[6] T. Inoue, S. Takaoka, and F. Adachi, "Frequency-domain equalization for MC-CDMA downlink site diversity and performance evaluation," IEICE Trans. Commun., vol.E88-B, no.1, pp.84–92, Jan. 2005.

[7] T. Ojanpera and R. Prasad, Wideband CDMA for third generation mobile communications, Artech House, 1998.

[8] T.S. Rappaport, Wireless communications, Prentice Hall, 1996.

Hirotaka Sato   received his B.S. and M.S. degrees in communications engineering from Tohoku University, Sendai, Japan, in 2005 and 2007. Since April 2007, he has been with Yokohama R&D center, Kyocera Corporation, Kanagawa, Japan. His research interests include frequency-domain equalization and site diversity techniques for mobile communication systems.

Hiromichi Tomeba   received his B.S. and M.S. degrees in communications engineering from Tohoku University, Sendai, Japan, in 2004 and 2006. Currently he is a Japan Society for the Promotion of Science (JSPS) research fellow, studying toward his PhD degree at the Department of Electrical and Communications Engineering, Graduate School of Engineering, Tohoku University. His research interests include frequency-domain equalization and antenna diversity techniques for mobile communication systems. He was a recipient of the 2004 and 2005 IEICE RCS (Radio Communication Systems) Active Research Award.

Kazuaki Takeda   received his B.E., M.S. and Dr. Eng. degrees in communications engineering from Tohoku University, Sendai, Japan, in 2003, 2004 and 2007, respectively. Currently he is a postdoctoral fellow at the Department of Electrical and Communications Engineering, Graduate School of Engineering, Tohoku University. Since 2005, he has been a Japan Society for the Promotion of Science (JSPS) research fellow. His research interests include equalization, interference cancellation, transmit/receive diversity, and multiple access techniques. He was a recipient of the 2003 IEICE RCS (Radio Communication Systems) Active Research Award and 2004 Inose Scientific Encouragement Prize.

Fumiyuki Adachi   received the B.S. and Dr. Eng. degrees in electrical engineering from Tohoku University, Sendai, Japan, in 1973 and 1984, respectively. In April 1973, he joined the Electrical Communications Laboratories of Nippon Telegraph & Telephone Corporation (now NTT) and conducted various types of research related to digital cellular mobile communications. From July 1992 to December 1999, he was with NTT Mobile Communications Network, Inc. (now NTT DoCoMo, Inc.), where he led a research group on wideband/broadband CDMA wireless access for IMT-2000 and beyond. Since January 2000, he has been with Tohoku University, Sendai, Japan, where he is a Professor of Electrical and Communication Engineering at the Graduate School of Engineering. His research interests are in CDMA wireless access techniques, equalization, transmit/receive antenna diversity, MIMO, adaptive transmission, and channel coding, with particular application to broadband wireless communications systems. From October 1984 to September 1985, he was a United Kingdom SERC Visiting Research Fellow in the Department of Electrical Engineering and Electronics at Liverpool University. He was a co-recipient of the IEICE Transactions best paper of the year award 1996 and again 1998 and also a recipient of Achievement award 2003. He is an IEEE Fellow and was a co-recipient of the IEEE Vehicular Technology Transactions best paper of the year award 1980 and again 1990 and also a recipient of Avant Garde award 2000. He was a recipient of Thomson Scientific Research Front Award 2004.